Analog Filter Design for Harmonic Reduction in Wind Energy Conversion System

VIKAS KUMAR SHARMA
Electrical Engineering Department
Global Institute of Technology
ITS-1, IT Park, EPIP, Sitapura, Jaipur
INDIA
vikasvs09@yahoo.co.in

LATA GIDWANI
Electrical Engineering Department
University College of Engineering
Rajasthan Technical Department, Kota
INDIA
lata_gidwani@rediffmail.com

Abstract: - These days Harmonics is major Power Quality concern for the Power system engineers. The multi-component, complex and dynamic power system has serious issues of harmonics which makes system nonlinear. The harmonics in the wind energy conversion system is mainly caused by non-liner loading effect from the power electronics converters and non-liner load. This paper presents an efficient analog filter combination for harmonic reduction of a grid integrated wind energy conversion system using Permanent Magnet Synchronous Generator (PMSG). The main purpose of the analog filter combination is to reduce Total Harmonic Distortion (THD) at different buses. Various combinations are taken using different analog filters and designing methods. These combinations are used at 575V, 25 KV, 120 KV buses and results are taken during normal as well as faulty conditions. The results are analysed for different faults at 575V bus and best combinations are suggested 575V, 25 KV, 120 KV buses.

Key-Words: - Wind Energy Conversion System, analog filter, harmonic reduction, Total Harmonic Reduction (THD), Permanent Magnet Synchronous Generator (PMSG).

1 Introduction

Wind energy conversion systems are the fastest growing renewable source of electrical energy having tremendous environmental, social, and economic benefits [1]. Power quality in wind energy conversion systems has also been a growing concern in recent years with many researches done in this area [2-3]. Harmonic emissions are recognized as a power quality problem for modern variable-speed wind turbines (WTs). For this reason, relevant standards [4] require the measurement of harmonics and their inclusion in the power quality certificates of WTs, and grid interconnection assessment procedures always comprise provisions for their control [5].

Yet, although a vast number of wind power stations are already in operation worldwide, relatively scarce literature exists to provide field-measurement-based information on the expected harmonic emission levels of real machines or to analysed their characteristics [6-7]. Understanding the harmonic behaviour of WTs is essential in order to analyse their effect on the grids where they are connected [8-9]. Detection and precise extraction of the compensating signal are the most important parts of a grid connected converter's control [10-13]. In high power applications, the harmonic content of the output waveforms has to be reduced as much as possible.

Wind energy conversion systems are the fastest growing renewable source of electrical energy having tremendous environmental, social, and economic benefits [1]. Power quality in wind energy conversion systems has also been a growing concern in recent years with many researches done in this area [2-3]. Harmonic emissions are recognized as a power quality problem for modern variable-speed wind turbines

(WTs). For this reason, relevant standards [4] require the measurement of harmonics and their inclusion in the power quality certificates of WTs, and grid interconnection assessment procedures always comprise provisions for their control [5].

Yet, although a vast number of wind power stations are already in operation worldwide, relatively scarce literature exists to provide field-measurement-based information on the expected harmonic emission levels of real machines or to analyse their characteristics [6-7]. Understanding the harmonic behaviour of WTs is essential in order to analyse their effect on the grids where they are connected [8-9]. Detection and precise extraction of the compensating signal are the most important parts of a grid connected converter's control [10-13]. In high power applications, the harmonic content of the output waveforms has to be reduced as much as possible.

These combinations are used at 575V, 25 KV, 120 KV buses and results are taken during normal as well as faulty conditions. The paper is divided into five sections. In section II and section III, wind farm model using PMSG and power system model simulations are discussed. Results and discussions are presented in Section IV. Conclusions are outlined in Section V and references are shown in Section VI.

2 PMSG Modelling

With large-scale exploration and integration of wind sources, variable speed wind turbine generators, PMSGs [14-16] are emerging as the preferred technology. In contrast to their fixed speed counterparts, the variable speed generators allow operating wind turbines at the optimum tip-speed ratio. The electrical model of PMSG in the synchronous reference frame is given in literature [17-18]. The electrical model of PMSG is shown in Fig. 1 and Fig. 2. The design parameters of PMSG are shown in Table 1.

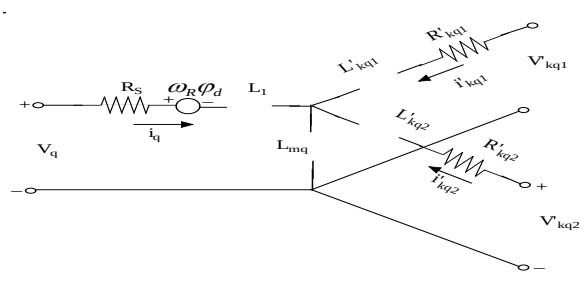

Fig. 1, q-Axis Electrical Model of PMSG

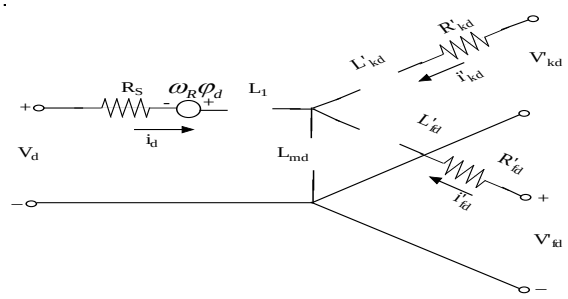

Fig. 2, d-Axis Electrical Model of PMSG

Following are the equations used in modelling of PMSG

$$V_d = R_s i_d + \frac{d\varphi_d}{dt} - \omega_r \varphi_q \quad (1)$$

$$V_q = R_s i_q + \frac{d\varphi_q}{dt} + \omega_r \varphi_d \quad (2)$$

$$V'_{fd} = R'_{fd} i'_{fd} + \frac{d\varphi'_{fd}}{dt} \quad (3)$$

$$V'_{kd} = R'_{kd} i'_{kd} + \frac{d\ddot{o}'_{kd}}{dt} \quad (4)$$

$$V'_{kq1} = R'_{kq1} i'_{kq1} + \frac{d\varphi'_{kq1}}{dt} \quad (5)$$

$$V'_{kq2} = R'_{kq2} i'_{kq2} + \frac{d\varphi'_{kq2}}{dt} \quad (6)$$

$$\varphi_d = L_d i_d + L_{md}\left(i'_{fd} + i'_{kd}\right) \quad (7)$$

$$\varphi_q = L_q i_q + L_{mq}\, i'_{kq} \quad (8)$$

$$\varphi'_{fd} = L'_{fd} i'_{fd} + L_{md}\,(i_d + i'_{kd}) \quad (9)$$

$$\varphi'_{kd} = L'_{kd} i'_{kd} + L_{md}\left(i_d + i'_{fd}\right) \quad (10)$$

$$\varphi'_{kq1} = L'_{kq1} i'_{kq1} + L_{mq}\, i_q \quad (11)$$

$$\varphi'_{kq2} = L'_{kq2} i'_{kq2} + L_{mq}\, i_q \quad (12)$$

$$T_e = \varphi_d i_q + \varphi_q\, i_d \quad (13)$$

Where

V_q, V_d	q-Axis and d-Axis Voltages
R_s	Resistance of the Stator Windings
i_q, i_d	q-Axis and d-Axis Currents
φ_q, φ_d	q-Axis and d-Axis Fluxes
ω_r	Angular Velocity of the Rotor
V'_{fd} , V'_{kd}	d-Axis Field & Damper Winding Voltage
R'_{fd} , R'_{kd}	d-Axis Field & Damper Winding Resistance
i'_{fd} , i'_{kd}	d-Axis Field & Damper Winding Current

φ'_{fd} , φ'_{kd} d-Axis Field & Damper Winding Flux

L'_{fd} , L'_{kd} d-Axis Field & Damper Winding Inductance

V'_{kq1} , V'_{kq2} q-Axis Damper Winding O/P Circuit Voltage 1 and Voltage 2

R'_{kq1} , R'_{kq2} q-Axis Damper Winding O/P Circuit Resistance 1 and Resistance 2

i'_{kq1} , i'_{kq2} q-Axis Damper Winding O/P Circuit Current 1 and Current 2

φ'_{kq1} , φ'_{kq2} q-Axis Damper Winding O/P Flux 1 and Flux 2

L'_{kq1} , L'_{kq2} q-Axis Damper Winding O/P Circuit Inductance 1 and Inductance 2

L_q, L_d q-Axis and d-Axis Inductances

L_{mq}, L_{md} q-Axis and d-Axis Magnetizing Inductances

T_e Electromagnetic Torque

Mechanical system for the model is

$$\frac{d\omega_r}{dt} = \frac{1}{J}\,(T_e - F\omega_r - T_m\,) \qquad (14)$$

$$\frac{d\theta}{dt} = \omega_r \qquad (15)$$

where,

J Combined Inertia of Rotor and Load

F Combined Viscous Friction of Rotor and Load

θ Rotor Angular Position

T_m Shaft Mechanical Torque

Table 1, Design Parameters of PMSG

Generator Data for Turbine	
Rated Electrical Power	2(MW)
Rated Mechanical Speed ($\omega_{g)}$	2.57(rd/s)
d-Axis Inductance, L_d	0.008(H)
q-Axis Inductance, L_q	0.0003(H)
Stator Resistance, R_s	0.0003(Ω)
Permanent Magnet Flux (Ψ_f)	0.4832Wb

3 Modelling Of WECS

The WECS considered for analysis consist of a PMSG driven by a wind turbine, rotor side converter and grid side converter, as shown in Fig. 3. Since the wind is the intermitted source of energy, the output voltage and frequency from generator will vary for different wind velocities. The variable output AC power from the generator is first converted into DC by rotor side converter. The available DC power is converted first to DC by intermediate circuit and then finally to AC by three phase PWM grid side inverter. The AC power is then fed to the grid at the required constant voltage and frequency.

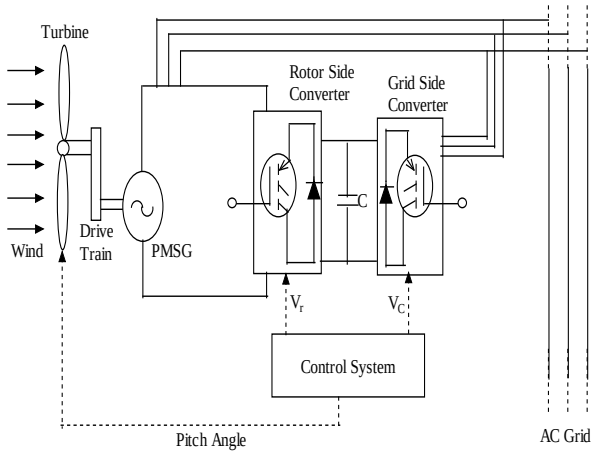

Fig. 3, Wind Energy Conversion System with PMSG and Conventional Converters

3.1 Rotor Side Converter

Rotor side converter consists of three phase IGBT-Diode rectifier connected in Graetz bridge configuration with snubber resistance and capacitance [19]. The power is controlled in order to follow a pre-defined power-speed characteristic, named tracking characteristic. The circuit is discretized at a sample time of 2 micro seconds. Fig.4 shows power, current and VAR regulation of rotor side converter.

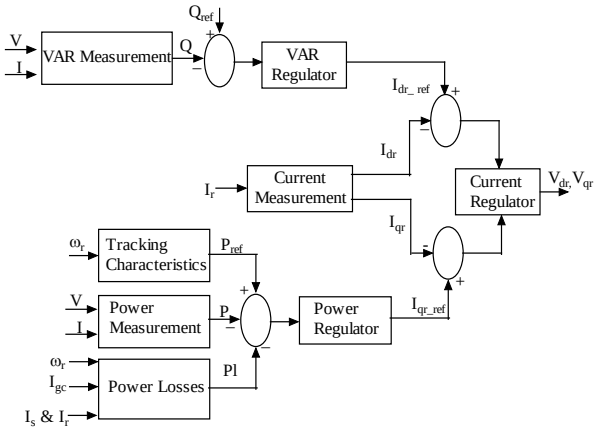

Fig. 4, Regulators of Rotor Side Converter

3.2 Grid Side Converter

Grid side converter also consists of three phase IGBT-Diode rectifier connected in Graetz bridge configuration as shown in Fig.5. The grid side converter is used to regulate the voltage of the DC bus capacitor. The pitch angle control is used to limit the power extracted at high wind speeds conditions.

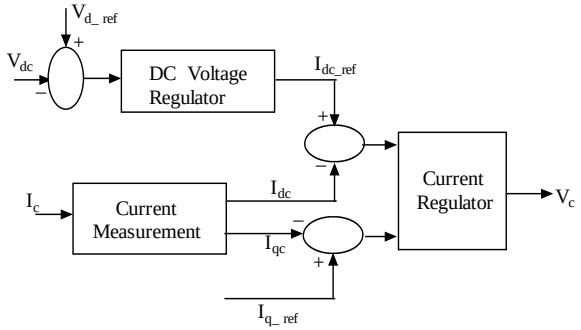

Fig. 5, Regulators of Grid Side Converter

3.3 Power Grid Model

The WECS is connected to a 575V distribution system exports power to a 120 KV grid through a 25 KV feeder as shown in Fig.6. WESE consists of a variable speed wind turbine, PMSG and AC-DC-AC IGBT based PWM converter.

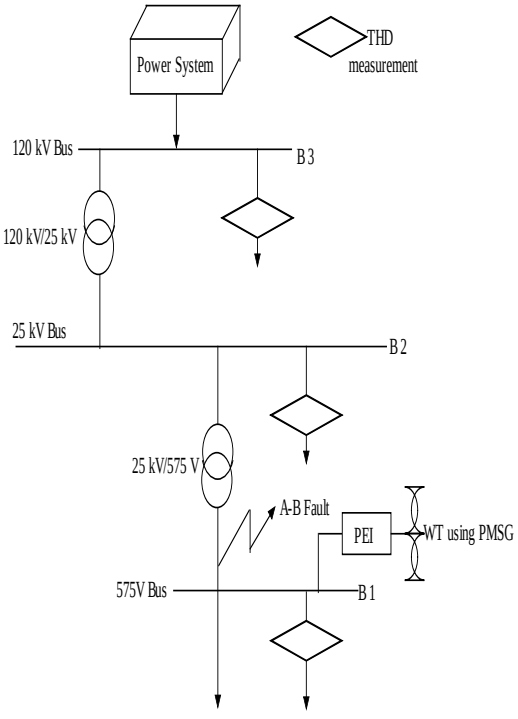

Fig. 6, Power System Model Integrated with Wind Farm

4 Results and Discussions

The observations are taken at different buses using various combinations of analog filter with different designing methods. Table 2 shows voltage THD values at 575V bus with different IIR analog filters and designing methods. Voltage THD before filter was found to be 3.48. It is seen that minimum THD obtained with IIR analog filter is 3.32 with bandpass filter designed with least pth norm method. Table 3 shows voltage THD values at 575V bus with different FIR analog filters and designing methods. It is seen that minimum THD obtained with FIR analog filter is 3.20 with multiband filter designed with least squares method. Hence voltage THD values at 575V bus are minimum with multiband filter designed with least squares method.

Table 2, Voltage THD Values at 575V Bus with Different IIR Analog Filters and Designing Methods

Response type/Design method	Butter worth	Least pth norm	Constr. Least pth norm	Cheby shev type 1	Cheby shev type 2	Elliptic	Maxi mally flat
Lowpass	3.48	3.48	3.48	3.53	3.48	3.51	3.48
Highpass	High THD	20.08	14.6	High THD	42.33	46.88	
Bandpass	High THD	3.32	872	High THD	High THD	High THD	
Bandstop	3.48	3.48	3.48	3.48	3.48	3.48	
Arbitrary Magnitude		3.48	3.48				
Arbitrary Group Delay			3.48				

Table 3, Voltage THD Values at 575V Bus with Different FIR Analog Filters and Designing Methods

Response type/Design method	Equir ipple	Least squares method	Window	Constr. Least squares	Least pth norm	Constrained Equir ipple	Generalised Equir ipple	Constr. Band Equir ipple
Lowpass	3.49	3.48	3.48	3.48	3.56	3.49	3.49	3.49
Raised cosine			3.47					
Halfband lowpass	3.47		3.47					
Nyquist	3.68		3.47					

Inv. Sinc Lowpass						3.49		
Highpass	3.43	3.63	3.53	3.49	3.24	1.10	3.43	3.43
Halfband highpass	3.29		3.27					
Inv. Sinc highpass						1.18		
Bandpass	3.32	3.27	3.29	3.28	3.32		3.32	3.32
Bandstop	3.52	3.51	3.52	3.50	3.43		3.52	3.52
Differentiator	2.80	2.85					2.80	2.90
Multiband	3.46	3.20		3.30			3.43	3.43
Hilbert Transformer	273	276						
Arbitrary Magnitude	3.43	3.46			3.48		3.43	3.43
Arbitrary Magnitude		2.7	2.7					
Arbitrary Group Delay			2.7					

Table 4 shows current THD values at 575V bus with different IIR analog filters and designing methods. Current THD before filter was found to be 2.7. It is seen that minimum THD obtained with IIR analog filter is 2.57 with highpass filter designed with Chebyshev type 2 method. Table 5 shows current THD values at 575V bus with different FIR analog filters and designing methods. It is seen that minimum THD obtained with FIR analog filter is 1.76 with bandpass filter designed with Generalised Equiripple (FIR) method. Hence current THD values at 575V bus is minimum with bandpass filter designed with Generalised Equiripple (FIR) method.

Table 4, Current THD Values at 575V Bus with Different IIR Analog Filters and Designing Methods

Response type/Design method	Butterworth	Least pth norm	Constr. Least pth norm	Chebyshev type 1	Chebyshev type 2	Elliptic	Maximally flat
Lowpass	2.7	2.7	2.7	2.75	2.7	2.72	2.7
Highpass	High THD	2.59	2.75	High THD	2.57	2.66	
Bandpass	High THD	29.6	21.9	High THD	73.1	62.1	
Bandstop	2.7	2.7	2.7	2.7	2.7	2.7	

Table 5, Current THD Values at 575V Bus with Different FIR Analog Filters and Designing Methods

Response type/Design method	Equiripple	Least squares method	Window	Constr. Least squares	Least pth norm	Constrained Equiripple	Generalised Equiripple	Constr. Band Equiripple
Lowpass	2.71	2.7	2.7	2.7	2.77	2.71	2.84	2.71
Raised cosine			2.69					
Halfband lowpass	2.69		2.69					
Nyquist	2.86		2.69					
Inv. Sinc Lowpass						2.71		
Highpass	2.66	2.74	2.69	2.68	2.48	2.43	2.66	2.66
Halfband highpass	2.53		2.50					
Inv. Sinc highpass						2.12		
Bandpass	2.55	2.51	2.53	2.52	2.56		1.76	2.55
Bandstop	2.74	2.73	2.73	2.72	2.66		2.74	2.74
Differentiator	2.26	2.28					2.26	2.28
Multiband	2.68	2.43		2.54			2.66	2.66
Hilbert Transformer	2.25	2.26						
Arbitrary Magnitude	2.66	2.68			2.7		2.66	2.66

Table 6 shows voltage THD values at 25 KV bus with different IIR analog filters and designing methods. Voltage THD before filter was found to be 5.72. It is seen that minimum THD obtained with IIR analog filter is 5.32 with highpass filter designed with Chebyshev type 2 method. Table 7 shows voltage THD values at 25 KV bus with different FIR analog filters and designing methods. It is seen that minimum THD obtained with FIR analog filter is 2.99 with inverse sinc

highpass filter designed with Constrained Equiripple (FIR) method. Hence voltage THD values at 25 KV bus is minimum with inverse sinc highpass filter designed with Constrained Equiripple (FIR) method.

Table 6, Voltage THD Values at 25KV Bus with Different IIR Analog Filters and Designing Methods

Response type/Design method	Butterworth	Least pth norm	Constr. Least pth norm	Chebyshev type 1	Chebyshev type 2	Elliptic	Maximally flat
Lowpass	5.72	5.72	5.72	5.87	5.72	5.79	5.72
Highpass	High THD	5.38	5.88	High THD	5.32	5.6	
Bandpass	High THD	35.84	545	High THD	567	565	
Bandstop	5.72	5.73	5.72	5.71	5.72	5.71	
Arbitrary Magnitude		5.72	5.71				
Arbitrary Group Delay			5.72				

Table 7, Voltage THD Values at 25KV Bus with Different FIR Analog Filters and Designing Methods

Response type/Design method	Equiripple (FIR)	Least squares method	Window	Constr. Least squares	Least pth norm	Constrained Equiripple	Generalised Equiripple	Constr. Band Equiripple
Lowpass	5.74	5.72	5.72	5.72	5.92	5.74	6.12	5.74
Raised cosine			5.69					
Halfband lowpass	5.69		5.69					
Nyquist	6.2		5.7					
Inv. Sinc Lowpass						5.75		
Highpass	5.59	5.85	5.74	5.67	5.06	4.21	5.59	5.59
Halfband highpass	5.2		5.13					
Inv. Sinc highpass						2.99		
Bandpass	5.29	5.15	5.2	5.17	5.30		5.29	5.29
Bandstop	5.83	5.80	5.82	5.78	5.60		5.83	5.83
Differentiator	5.61	5.64					5.61	5.66
Multiband	5.66	4.91		5.24			5.6	5.6
Hilbert Transformer	5.58	5.60						
Arbitrary Magnitude	5.6	5.67			5.72		5.6	5.6

Table 8 shows current THD values at 25 KV bus with different IIR analog filters and designing methods. Current THD before filter was found to be 1.98. It is seen that minimum THD obtained with IIR analog filter is 1.93 with highpass filter designed with Least pth norm method or highpass filter designed with Chebyshev type 2 method. Table 9 shows current THD values at 25 KV bus with different FIR analog filters and designing methods. It is seen that minimum THD obtained with FIR analog filter is 1.67 with inverse sinc highpass filter designed with Constrained Equiripple (FIR) method. Hence current THD values at 25 KV bus is minimum with inverse sinc highpass filter designed with Constrained Equiripple (FIR) method.

Table 8, Current THD Values at 25KV Bus with Different IIR Analog Filters and Designing Methods

Response type/Design method	Butterworth	Least pth norm	Constr. Least pth norm	Chebyshev type 1	Chebyshev type 2	Elliptic	Maximally flat
Lowpass	1.98	1.98	1.98	2.00	1.98	1.99	1.98
Highpass	High THD	1.93	2.00	High THD	1.93	1.96	
Bandpass	High THD	7.97	12.0	High THD	12.5	12.4	
Bandstop	1.98	1.98	1.98	1.98	1.98	1.98	
Arbitrary Magnitude		1.98	1.98				
Arbitrary Group Delay			1.98				
Peaking							
Notching							

Table 9, Current THD Values at 25KV Bus with Different FIR Analog Filters and Designing Methods

Response type/Design method	Equiripple	Least squares method	Window	Constr. Least squares	Least pth norm	Constrained Equiripple	Generalised Equiripple	Constr. Band Equiripple
Lowpass	1.98	1.98	1.98	1.98	2.01	1.98	2.04	1.98
Raised cosine			1.98					
Halfband lowpass	1.98		1.98					
Nyquist	2.05		1.98					
Inv. Sinc Lowpass						1.99		
Highpass	1.96	2.00	1.98	1.97	1.89	1.79	1.96	1.96
Halfband highpass	1.91		1.90					
Inv. Sinc highpass						1.67		
Bandpass	1.92	1.9	1.91	1.91	1.92		1.92	1.92
Bandstop	2.00	1.99	1.99	1.99	1.96		2.00	2.00
Differentiator	1.23	1.24					1.23	1.25
Multiband	1.97	1.87		1.92			1.96	1.96
Hilbert Transformer	123	123						
Arbitrary Magnitude	1.96	1.97			1.98		1.96	1.96

Table 10 shows voltage THD values at 120 KV bus with different IIR analog filters and designing methods. Voltage THD before filter was found to be 0.6. It is seen that minimum THD obtained with IIR analog filter is 0.56 with highpass filter designed with Chebyshev type 2 method. Table 11 shows voltage THD values at 120 KV bus with different FIR analog filters and designing methods. It is seen that minimum THD obtained with FIR analog filter is 0.26 with bandpass filter designed with Generalised Equiripple (FIR) method. Hence voltage THD values at 120 KV bus is minimum with bandpass filter designed with Generalised Equiripple (FIR) method.

Table 10, Voltage THD Values at 120KV Bus with Different IIR Analog Filters and Designing Methods

Response type/Design method	Butterworth	Least pth norm	Constr. Least pth norm	Chebyshev type 1	Chebyshev type 2	Elliptic	Maximally flat
Lowpass	0.6	0.6	0.6	0.62	0.6	0.61	0.6
Highpass	High THD	0.57	0.62	High THD	0.56	0.59	
Bandpass	High THD	3.77	5.74	High THD	6.0	5.95	
Bandstop	0.6	0.6	0.6	0.6	0.6	3.48	
Arbitrary Magnitude		0.6	0.6				
Arbitrary Delay			0.6				

Table 11: Voltage THD Value at 120KV Bus with Different FIR Analog Filters and Designing Methods

Response type/Design method	Equiripple	Least squares method	Window	Constr. Least squares	Least pth norm	Constrained Equiripple	Generalised Equiripple	Constr. Band Equiripple
Lowpass	0.6	0.6	0.6	0.6	0.62	0.6	0.64	0.6
Raised cosine			0.6					
Halfband lowpass	0.6		0.6					
Nyquist	0.65		0.6					
Inv. Sinc Lowpass						0.61		
Highpass	0.59	0.62	0.6	0.6	0.53	0.44	0.59	0.59
Halfband highpass	0.55		0.54					
Inv. Sinc highpass						0.31		
Bandpass	0.56	0.54	0.55	0.54	0.56		0.26	0.56
Bandstop	0.61	0.61	0.61	0.61	0.59		0.61	0.61
Differentiator	5.9	5.9					5.9	6.0
Multiband	0.6	0.52		0.55			0.59	0.59

Hilbert Transformer	5.9	5.9						
Arbitrary Magnitude	0.59	0.6			0.6		0.59	0.59

Table 12 shows current THD values at 120 KV bus with different IIR analog filters and designing methods. Current THD before filter was found to be 1.78. It is seen that minimum THD obtained with IIR analog filter is 1.71 with highpass filter designed with Chebyshev type 2 method. Table 13 shows current THD values at 120 KV bus with different FIR analog filters and designing methods. It is seen that minimum THD obtained with FIR analog filter is 1.34 with bandpass filter designed with Generalised Equiripple (FIR) method. Hence current THD values at 120 KV bus is minimum with bandpass filter designed with Generalised Equiripple (FIR) method.

Table 12, Current THD Values at 120KV Bus with Different IIR Analog Filters and Designing Methods

Response type/Design method	Butterworth	Least pth norm	Constr. Least pth norm	Chebyshev type 1	Chebyshev type 2	Elliptic	Maximally flat
Lowpass	1.78	1.78	1.78	1.8	1.78	1.79	1.78
Highpass	High THD	1.72	1.80	High THD	1.71	1.76	
Bandpass	High THD	8.03	121	High THD	124	125	
Bandstop	1.78	1.78	1.78	1.78	1.78	3.48	
Arbitrary Magnitude		1.78	1.78				
Arbitrary Group Delay			1.78				
Peaking							
Notching							

Table 13, Current THD Values at 120KV Bus with Different FIR Analog Filters and Designing Methods

Response type/Design method	Equiripple	Least squares method	Window	Constr. Least squares	Least pth norm	Constrained Equiripple	Generalised Equiripple	Constr. Band Equiripple
Lowpass	1.78	1.78	1.78	1.78	1.81	1.78	1.84	1.78
Raised cosine			1.77					
Halfband lowpass	1.77		1.77					
Nyquist	1.85		1.77					
Inv. Sinc Lowpass						1.78		
Highpass	1.76	1.80	1.78	1.77	1.67	1.55	1.76	1.76
Halfband highpass	1.7		1.69					
Inv. Sinc highpass						1.41		
Bandpass	1.71	1.69	1.70	1.69	1.71		1.34	1.71
Bandstop	1.8	1.79	1.79	1.79	1.76		1.80	1.8
Differentiator	12.5	12.5					12.5	12.6
Multiband	1.77	1.65		1.70			1.76	1.76
Hilbert Transformer	124	125						
Arbitrary Magnitude	1.76	1.77			1.78		1.76	1.76

Table 14 and Table 15 show voltage THD and current THD values at different buses with different combinations of response type and design method used respectively. The various combinations of analog filters designed with suitable designing methods C1 to C20 are provided at the end of table. It is observed that combination C1 and C12 are best among all combinations as voltage THD and current THD values are least in these combinations. Table 16 and Table 17 show voltage THDs and current THDs with C1 and C12 during different faults at 575V bus respectively.

Table 14, Voltage THD Values at Different Buses with Different Combinations Used

Combinations	Voltage THD					
	575V Bus		25KV Bus		120KV Bus	
	bfc	afc	bfc	afc	bfc	afc
C1	3.48	3.2	5.72	2.99	0.59	0.26
C2	3.48	3.2	5.72	2.99	0.59	0.31
C3	3.48	3.2	5.72	4.21	0.59	0.31
C4	3.48	3.2	5.72	4.21	0.59	0.26
C5	3.48	3.27	5.72	4.21	0.59	0.26
C6	3.48	3.27	5.72	4.21	0.59	0.26
C7	3.48	3.27	5.72	4.21	0.59	0.31
C8	3.48	3.27	5.72	4.21	0.59	0.31
C9	3.48	3.27	5.72	2.99	0.59	0.31
C10	3.48	3.27	5.72	2.99	0.59	0.31
C11	3.48	3.27	5.72	2.99	0.59	0.26
C12	3.48	3.27	5.72	2.99	0.59	0.26
C13	3.48	14.78	5.72	2.99	0.59	0.26
C14	3.48	14.78	5.72	2.99	0.59	0.31
C15	3.48	14.78	5.72	4.21	0.59	0.31
C16	3.48	14.78	5.72	4.21	0.59	0.26
C17	3.48	118	5.72	4.21	0.59	0.26
C18	3.48	118	5.72	4.21	0.59	0.31
C19	3.48	118	5.72	2.99	0.59	0.31
C20	3.48	118	5.72	2.99	0.59	0.26

Table 15, Current THD Values at Different Buses with Different Combinations Used

Combinations	Current THD					
	575V Bus		25KV Bus		120KV Bus	
	bfc	afc	bfc	afc	bfc	afc
C1	2.7	2.43	1.98	1.67	1.77	1.34
C2	2.7	2.43	1.98	1.67	1.77	1.4
C3	2.7	2.43	1.98	1.79	1.77	1.4
C4	2.7	2.43	1.98	1.79	1.77	1.34
C5	2.7	2.5	1.98	1.79	1.77	1.34
C6	2.7	2.51	1.98	1.79	1.77	1.34
C7	2.7	2.5	1.98	1.79	1.77	1.4
C8	2.7	2.51	1.98	1.79	1.77	1.4
C9	2.7	2.5	1.98	1.67	1.77	1.4
C10	2.7	2.51	1.98	1.67	1.77	1.4
C11	2.7	2.51	1.98	1.67	1.77	1.34
C12	2.7	2.5	1.98	1.67	1.77	1.34
C13	2.7	1.76	1.98	1.67	1.77	1.34
C14	2.7	1.76	1.98	1.67	1.77	1.4
C15	2.7	1.76	1.98	1.79	1.77	1.4
C16	2.7	1.76	1.98	1.79	1.77	1.34
C17	2.7	2.12	1.98	1.79	1.77	1.34
C18	2.7	2.12	1.98	1.79	1.77	1.4
C19	2.7	2.12	1.98	1.67	1.77	1.4
C20	2.7	2.12	1.98	1.67	1.77	1.34

C1 : Multiband and Least squares method (FIR) at 575V bus; Inv. Sinc highpass and Constrained Equiripple (FIR) at 25KV bus; Bandpass and Generalised Equiripple (FIR) at 120KV bus.
C2 : Multiband and Least squares method (FIR) at 575Vbus; Inv. Sinc highpass and Constrained Equiripple (FIR) at 25KV bus; Inv. Sinc highpass and Constrained Equiripple (FIR) at 120KV bus.
C3 : Multiband and Least squares method (FIR) at 575Vbus; Highpass and Constrained Equiripple (FIR) at 25KV bus; Inv. Sinc highpass and Constrained Equiripple (FIR) at 120KV bus.
C4 : Multiband and Least squares method (FIR) at 575Vbus; Highpass and Constrained Equiripple (FIR) at 25KV bus; Bandpass and Generalised Equiripple (FIR) at 120KV bus.
C5 : Halfband highpass and Window (FIR) at 575Vbus; Highpass and Constrained Equiripple (FIR) at 25KV bus; Bandpass and Generalised Equiripple (FIR) at 120KV bus.
C6 : Bandpass and Least squares method (FIR) at 575Vbus; Highpass and Constrained Equiripple (FIR) at 25KV bus; Bandpass and Generalised Equiripple (FIR) at 120KV bus.
C7 : Halfband highpass and Window (FIR) at 575Vbus; Highpass and Constrained Equiripple (FIR) at 25KV bus; Inv. Sinc highpass and Constrained Equiripple (FIR) at 120KV bus.
C8 : Bandpass and Least squares method (FIR) at 575Vbus; Highpass and Constrained Equiripple (FIR) at 25KV bus; Inv. Sinc highpass and Constrained Equiripple (FIR) at 120KV bus.
C9 : Halfband highpass and Window (FIR) at 575Vbus; Inv. Sinc highpass and Constrained Equiripple (FIR) at 25KV bus; Inv. Sinc highpass and Constrained Equiripple (FIR) at 120KV bus.
C10 : Bandpass and Least squares method (FIR) at 575Vbus; Inv. Sinc highpass and Constrained Equiripple (FIR) at 25KV bus; Inv. Sinc highpass and Constrained Equiripple (FIR) at 120KV bus.
C11 : Bandpass and Least squares method (FIR) at 575Vbus; Inv. Sinc highpass and Constrained Equiripple (FIR) at 25KV bus; Bandpass and Generalised Equiripple (FIR) at 120KV bus.
C12 : Halfband highpass and Window (FIR) at 575Vbus; Inv. Sinc highpass and Constrained Equiripple (FIR) at 25KV bus; Bandpass and Generalised Equiripple (FIR) at 120KV bus.
C13 : Bandpass and Generalised Equiripple (FIR) at 575Vbus; Inv. Sinc highpass and Constrained Equiripple (FIR) at 25KV bus; Bandpass and Generalised Equiripple (FIR) at 120KV bus.
C14 : Bandpass and Generalised Equiripple (FIR) at 575Vbus; Inv. Sinc highpass and Constrained Equiripple (FIR) at 25KV bus; Inv. Sinc highpass and Constrained Equiripple (FIR) at 120KV bus.
C15 : Bandpass and Generalised Equiripple (FIR) at 575Vbus; Highpass and Constrained Equiripple (FIR) at 25KV bus; Inv. Sinc highpass and Constrained Equiripple (FIR) at 120KV bus.
C16 : Bandpass and Generalised Equiripple (FIR) at 575Vbus; Highpass and Constrained Equiripple (FIR) at 25KV bus; Bandpass and Generalised Equiripple (FIR) at 120KV bus.
C17 : Inv. Sinc highpass and Constrained Equiripple (FIR) at 575Vbus; Highpass and Constrained Equiripple (FIR) at 25KV bus;

Bandpass and Generalised Equiripple (FIR) at 120KV bus.
C18 : Inv. Sinc highpass and Constrained Equiripple (FIR) at 575Vbus; Highpass and Constrained Equiripple (FIR) at 25KV bus; Inv. Sinc highpass and Constrained Equiripple (FIR) at 120KV bus.
C19 : Inv. Sinc highpass and Constrained Equiripple (FIR) at 575Vbus; Inv. Sinc highpass and Constrained Equiripple (FIR) at 25KV bus; Inv. Sinc highpass and Constrained Equiripple (FIR) at 120KV bus.
C20 : Inv. Sinc highpass and Constrained Equiripple (FIR) at 575Vbus; Inv. Sinc highpass and Constrained Equiripple (FIR) at 25KV bus; Bandpass and Generalised Equiripple (FIR) at 120KV bus.

Table 16, Voltage THDs with C1 and C12 during Different Faults at 575V Bus

	Voltage THD					
Fault at 575V Bus with C1	575V Bus		25KV Bus		120KV Bus	
	bfc	afc	bfc	afc	bfc	afc
Phase to Ground	3.79	3.48	6.36	3.32	0.66	0.29
Phase to Phase	3.94	3.64	6.58	3.44	0.68	0.3
Phase to Phase to ground	4.37	4.07	6.8	3.54	0.71	0.31
Three phase	4.21	3.88	7.12	3.7	0.74	0.32
Three phase to ground	4.35	4.03	7.13	3.72	0.74	0.32
Fault at 575V Bus with C12	575V Bus		25KV Bus		120KV Bus	
	bfc	afc	bfc	afc	bfc	afc
Phase to Ground	3.79	3.48	6.36	3.32	0.66	0.29
Phase to Phase	3.94	3.64	6.58	3.44	0.68	0.3
Phase to Phase to ground	4.37	4.07	6.8	3.54	0.71	0.31
Three phase	4.21	3.88	7.12	3.7	0.74	0.32
Three phase to ground	4.35	4.03	7.13	3.72	0.74	0.32

Table 17, Current THDs with C1 and C12 during Different Faults at 575V Bus

	Current THD					
Fault at 575V Bus with C1	575V Bus		25KV Bus		120KV Bus	
	bfc	afc	bfc	afc	bfc	afc
Phase to Ground	2.87	2.56	2.03	1.58	2.16	1.73
Phase to Phase	3.03	2.72	2.42	2.03	2.08	1.61
Phase to Phase to ground	3.27	2.95	2.13	1.65	2.96	2.63
Three phase	3.18	2.83	2.07	1.52	2.51	2.07
Three phase to ground	3.29	2.95	2.3	1.81	2.57	2.15
Fault at 575V Bus with C12	575V Bus		25KV Bus		120KV Bus	
	bfc	afc	bfc	afc	bfc	afc
Phase to Ground	2.87	2.65	2.03	1.64	2.16	1.73
Phase to Phase	3.03	2.81	2.42	2.08	2.08	1.61
Phase to Phase to ground	3.27	3.04	2.13	1.71	2.96	2.63
Three phase	3.18	2.92	2.07	1.59	2.51	2.07
Three phase to ground	3.29	3.04	2.3	1.87	2.57	2.15

bfc:before filter combination
afc:after filter combination

It is observed that voltage THDs and current THDs rise above specified limits during faults, but with filter combinations C1 and C12, voltage THDs and current THDs fall below specified limits. Comparatively, looking at THD values, combination C1 is better than C12. Hence it is concluded that among different analog filters with various designing methods, Multiband and Least squares method (FIR) at 575V bus; Inv. Sinc highpass and Constrained Equiripple (FIR) at 25KV bus; Bandpass and Generalised Equiripple (FIR) at 120KV bus is the best combination.

5. Conclusions

Harmonics analysis is an essential part of the grid impact studies needed for new wind farms. That can lead to the earlier detection of potential series and parallel resonance problems. Consequently, a harmonics mitigation solution is examined in this paper. The simulated results on transients of a power system grid integrated with wind power are presented. In this paper, we attempted to compare the impact, in terms of voltage THDs and currents THDs, of adding analog filters to wind integrated power system consisting of PMSG. Various analog filters are designed using different designing methods and then the effect of adding them to various buses is examined. The results have clearly demonstrated the ability of analog filters to reduce transients and harmonic distortion in power system. It is concluded that among different analog filters with various designing methods, Multiband and Least squares method (FIR) at 575V bus; Inv. Sinc highpass and Constrained Equiripple (FIR) at 25KV bus; Bandpass and Generalised Equiripple (FIR) at 120KV bus is the best combination. As a future scope of this work the proposed combination of analog filter can be implemented practically to show the validation of work also the designed filters can be used other renewable sources integration as they are injecting harmonics in to the system.

References:

[1]. S.W Mohod, M.V Aware, "A STATCOM control scheme for grid connected wind energy system for power quality improvement", *IEEE System Journal*, Vol.2, issue 3, pp.346-352, Sept.2010

[2] H. Akagi, "Active Harmonic Filter," *Proceedings of the IEEE*, pp. 2128-2141, 2005.

[3] Rekik, M.; Krichen, L., "Active power filter based on wind turbine for electric power system quality improvement," *Multi-Conference on Systems, Signals & Devices (SSD)*, 2014 11th International , vol., no., pp.1,5, 11-14 Feb. 2014

[4] Lian, K. L. Noda, T.," A Time-Domain Harmonic Power-Flow Algorithm for Obtaining Nonsinusoidal Steady-State Solutions", *IEEE Transactions on Power Delivery*, Issue 99, 2010.

[5] S. A. Papathanassiou, "A Technical Evaluation Framework for the Connection of DG to the Distribution Network," *Electr. Power Syst. Res*., vol. 77, no. 1, pp. 24–34, Jan. 2007.

[6] Rekik, M.; Krichen, L., "Active power filter based on wind turbine for electric power system quality improvement," *Multi-Conference on Systems, Signals & Devices (SSD)*, 2014 11th International , vol. 1., no. 2., pp.1,5, 11-14 Feb. 2014

[7] T. Thiringer, T. Petru, and C. Liljegren, "Power Quality Impact of a Sea Located Hybrid Wind Park," *IEEE Trans. Energy Conversion*, vol. 16, no. 2, pp. 123–127, Jun. 2001.

[8] S. A. Papathanassiou and M. P. Papadopoulos, "Harmonic Analysis in a Power System with Wind Generation," *IEEE Trans. Power Del*., vol. 21, no. 4, pp. 2006–2016, Oct. 2006.

[9]Rekik, M.; Krichen, L., "Active power filter based on wind turbine for electric power system quality improvement," *Multi-Conference on Systems, Signals & Devices (SSD)*, 2014 11th International , vol., no., pp.1,5, 11-14 Feb. 2014

[10] V.M.Moreno, M. Liserre, A. Pigazo, and A. Dell'Aquila, "A Comparative Analysis of Real-Time Algorithms for Power SignalDecomposition in Multiple Synchronous Reference Frames," *IEEE Trans. Power Electron*., vol. 22, no. 4, pp. 1280–1289, Jul. 2007.

[11] R. S. Herrera, P. Salmeron, and H. Kim, "Instantaneous Reactive Power Theory Applied to Active Power Filter Compensation: Different Approaches, Assessment, and Experimental Results," *IEEE Trans. Ind. Electron*., vol. 55, no. 1, pp. 184–196, Jan. 2008.

[12] J. Rodriguez, S. Bernet, B. Wu, J. O. Pontt and S. Kouro, "Multilevel Voltage-Source-Converter Topologies for Industrial Medium-Voltage Drives," *IEEE Trans. Ind. Electron*., vol. 54, no. 6, pp. 2930–2945, Dec. 2007.

[13] L. G. Franquelo, J. Rodriguez, J. I. Leon, S. Kouro, R. Portillo and M.M. Prats, "The Age of Multilevel Converters Arrives,"*IEEE Ind. Electron. Magazine*, vol. 2, no. 2, pp. 28–39, June 2008.

[14] Yang G., Zhu Y., "Application of a Matrix Converter for PMSG Wind Turbine Generation System", *IEEE 2nd Int. Symposium on Power Electronics for Distributed Generation Systems (PEDG)*, Hefei, China, pp. 185-189, Jun. 16-18, 2010.

[15] Carrillo C., Diaz-Dorado E., Silva-Ucha M., Perez-Sabín F., "Effects of WECS Settings and PMSG Parameters in the Performance of a Small Wind Energy Generator", *Int. Symposium on Power Electronics Electrical Drives Automation and Motion (SPEEDAM)*, Pisa, pp. 766 – 771, Jun. 14-16, 2010.

[16] Wai R.J., Lin C.Y., Chang Y.R., "Novel Maximum-Power-Extraction Algorithm for PMSG Wind Generation System", *IET Electric Power Applications*, vol. 1, issue 2, pp.275-283, Mar. 2007.

[17] Rolan A., Luna A., Vazquez G., Aguilar D., Azevedo G., "Modeling of a Variable Speed Wind Turbine with a Permanent Magnet Synchronous Generator", *IEEE Int. Symposium on Industrial Electronics*, Seoul, Korea, pp. 734-739, Jul. 5-8, 2009.

[18] Chung S.K., "Phase-locked Loop for Grid-Connected Three-Phase Power Conversion Systems", *Proc. IEE Electronics Power Applications*, vol. 147, no. 3, pp. 213-219, May 2000.

[19] Lata Gidwani, Harpal Tiwari, R.C. Bansal, N. Mithulananthan, "Improving Power Quality of Wind Energy Conversion System with Efficient Power Electronic Interface", *International Journal of Electrical Power and Energy Systems*, Elsevier Publications, vol. 44, issue 1, pp. 445-452, 2013.